AMERICAN SOCIETY FOR MICROBIOLOGY | Applied and Environmental Microbiology®

GENETICS AND MOLECULAR BIOLOGY

In Vitro Evolution of *Listeria monocytogenes* Reveals Selective Pressure for Loss of SigB and AgrA Function at Different Incubation Temperatures

Duarte N. Guerreiro,[a] Jialun Wu,[a] Emma McDermott,[b] Dominique Garmyn,[d] Peter Dockery,[b] Aoife Boyd,[c] Pascal Piveteau,[e] Conor P. O'Byrne[a]

[a]Bacterial Stress Response Group, Microbiology, Ryan Institute, School of Biological and Chemical Sciences, National University of Ireland, Galway, Ireland
[b]Centre for Microscopy and Imaging, Anatomy School of Medicine, National University of Ireland, Galway, Ireland
[c]Pathogenic Mechanisms Research Group, Microbiology, School of Natural Sciences, National University of Ireland, Galway, Ireland
[d]Agroécologie, AgroSup Dijon, INRAE, University Bourgogne, University Bourgogne Franche-Comté, Dijon, France
[e]INRAE, UR OPAALE, Rennes, France

ABSTRACT The alternative sigma factor B (σ^B) contributes to the stress tolerance of the foodborne pathogen *Listeria monocytogenes* by upregulating the general stress response. We previously showed that σ^B loss-of-function mutations arise frequently in strains of *L. monocytogenes* and suggested that mild stresses might favor the selection of such mutations. In this study, we performed *in vitro* evolution experiments (IVEE) where *L. monocytogenes* was allowed to evolve over 30 days at elevated (42°C) or lower (30°C) incubation temperatures. Isolates purified throughout the IVEE revealed the emergence of *sigB* operon mutations at 42°C. However, at 30°C, independent alleles in the *agr* locus arose, resulting in the inactivation of Agr quorum sensing. Colonies of both *sigB* mutants and *agr* mutants exhibited a greyer coloration on 7-days-old agar plates than those of the parental strain. Scanning electron microscopy revealed a more complex colony architecture in the wild type than in the mutant strains. *sigB* mutant strains outcompeted the parental strain at 42°C but not at 30°C, while *agr* mutant strains showed a small increase in competitive fitness at 30°C. Analysis of 40,080 *L. monocytogenes* publicly available genome sequences revealed a high occurrence rate of premature stop codons in both the *sigB* and *agrCA* loci. An analysis of a local *L. monocytogenes* strain collection revealed 5 out of 168 strains carrying *agrCA* alleles. Our results suggest that the loss of σ^B or Agr confer an increased competitive fitness in some specific conditions and this likely contributes to the emergence of these alleles in strains of *L. monocytogenes*.

IMPORTANCE To withstand environmental aggressions, *L. monocytogenes* upregulates a large regulon through the action of the alternative sigma factor B (σ^B). However, σ^B becomes detrimental for *L. monocytogenes* growth under mild stresses, which confer a competitive advantage to σ^B loss-of-function alleles. Temperatures of 42°C, a mild stress, are often employed in mutagenesis protocols of *L. monocytogenes* and promote the emergence of σ^B loss-of-function alleles in the *sigB* operon. In contrast, lower temperatures of 30°C promote the emergence of Agr loss-of-function alleles, a cell-cell communication mechanism in *L. monocytogenes*. Our findings demonstrate that loss-of-function alleles emerge spontaneously in laboratory-grown strains. These alleles rise in the population as a consequence of the trade-off between growth and survival imposed by the activation of σ^B in *L. monocytogenes*. Additionally, our results demonstrate the importance of identifying unwanted hitchhiker mutations in newly constructed mutant strains.

KEYWORDS *Listeria monocytogenes*, *in vitro* evolution, σ^B, *agr* system, bacterial competition, general stress response, quorum sensing

Editor Edward G. Dudley, The Pennsylvania State University

Address correspondence to Conor P. O'Byrne, conor.obyrne@nuigalway.ie.

The authors declare no conflict of interest.

Received 21 February 2022
Accepted 15 April 2022
Published 18 May 2022

The Gram-positive bacterium *Listeria monocytogenes* is a robust foodborne pathogen found in a wide range of environments, such as soil, water, and feces from both animals and humans (reviewed in references 1 and 2). *L. monocytogenes* is the etiological agent of the disease listeriosis and is frequently associated with high mortality rates (typically 20 to 30%) (3). Listeriosis is especially hazardous for children, pregnant women, elderly people, and immunocompromised patients. To establish an infection, *L. monocytogenes* relies on its ability to withstand the extreme acidic pH of the stomach, as well as the osmotic stress and bile encountered in the duodenum (4–6).

The alternative sigma factor B (σ^B) is responsible for the transcriptional control of a large regulon (~300 genes or approximately 10% of *L. monocytogenes* genes), designated the general stress response (GSR) regulon, whose principal function is to protect against environmental stress (reviewed in reference 6–8). σ^B is also implicated in *L. monocytogenes* virulence by regulating the expression of the internalins *inlA* and *inlB* (9). These cell wall-associated proteins enhance *L. monocytogenes* invasion toward nonphagocytic cells at the intestinal epithelium (10, 11) through interactions with the E-cadherin and Met receptors, respectively (12, 13).

The activity of σ^B is controlled through a complex signal transduction cascade, where a stress-sensing protein complex known as the stressosome (composed of RsbR, RsbS, and RsbT) integrates environmental stress signals into the σ^B pathway. The current model proposes that following a stressful stimulus, the kinase RsbT phosphorylates RsbR and RsbS leading to the subsequent release of RsbT from the stressosome. Free RsbT then interacts with and activates the phosphatase activity of RsbU, whose substrate is the phosphorylated anti-anti-sigma factor RsbV. RsbV then sequesters RsbW, the anti-sigma factor that prevents σ^B from associating with RNA polymerase under nonstress conditions. The RsbV-RsbW interaction favors the association of σ^B with the RNA polymerase, to form the holoenzyme $E\sigma^B$ and, consequently, transcription of the GSR regulon. Once the stress conditions abate, or the cell has adequately responded to them, the stressosome is reset to a sensing-competent state through the action of the RsbX phosphatase, which reestablishes the appropriate phosphorylation state of RsbR and RsbS (14, 15). All the proteins involved in this signal cascade are encoded by the *sigB* operon, which comprises *rsbRSTUVW-sigB-rsbX* (16).

σ^B plays an important role in enhancing *L. monocytogenes* resistance toward a wide range of lethal stresses (reviewed in references 2, 7, 17). However, deploying σ^B under certain mildly stressful conditions comes with a cost, evidenced by an increase in growth rate for mutants lacking this sigma factor (18–20). Recently, we reported that mild heat stress (42°C) gives mutants lacking σ^B a competitive advantage in mixed cultures (21). Many of the genetic techniques used with *L. monocytogenes* rely on plasmids with a temperature-sensitive replication origin unable to replicate at temperatures above 37°C (e.g., *ori* pE194^{ts} in pMC39, a transposon delivery vector [22], and pMAD, a vector widely used for *L. monocytogenes* mutagenesis [23]). We also reported that the rate of premature stop codon (PMSC) occurrence in the *sigB* operon is unusually high, suggesting that sequenced strains might be subject to selective pressures for loss of σ^B function (21). Taken together, these observations suggested that mild stress during laboratory culture might select for σ^B loss-of-function mutations. The present study sought to investigate whether extended growth at elevated temperature (42°C) would give rise to mutations affecting σ^B activity.

In *L. monocytogenes*, quorum sensing (QS) is mediated by the Agr system, which is encoded by a four-gene operon (*agrBDCA*). AgrC (histidine kinase) and AgrA (response regulator) form a two-component system that senses the concentration of a signaling peptide that is encoded by *agrD* and secreted by AgrC (24). The Agr system is crucial for cell surface attachment and biofilm formation when *L. monocytogenes* is growing at lower temperatures (25 to 30°C) (25–27). Deletion of either the *agrA* or *agrD* genes in *L. monocytogenes* EGD-e results in significant changes in global gene expression in log-phase cultures. There is a significant overlap between the genes affected by the loss of Agr and the σ^B regulon, suggesting a regulatory connection between the general stress response and quorum sensing systems (25, 26, 28, 29).

In this study, *in vitro* evolution experiments (IVEE) were performed to determine whether mutations affecting σ^B activity were selected in populations passaged for a 30-day period at 42°C compared to control cultures grown at 30°C. A colony phenotype associated with loss of σ^B function was used to detect the emergence of potential *sigB* operon mutations in evolved populations; mutants lacking *sigB* have a grey colony phenotype (21). Whole-genome sequencing (WGS), performed on multiple isolates from both populations, revealed that *sigB* loss-of-function mutations arise at 42°C but not at 30°C. However, grey colony variants did emerge at 30°C but were found to harbor mutations in the *agr* operon, specifically in *agrA* and *agrC*, but not in the *sigB* operon. An analysis of the published genome sequences of over 40,000 *L. monocytogenes* strains revealed that *agrA* and *agrC* mutations occur at a high rate compared to the other two-component systems, suggesting a selective pressure. Our results show that loss-of-function mutations in both the *sigB* and *agr* operons can be selected during routine laboratory culture. Both the σ^B and Agr systems can influence colony architecture as indicated by scanning electron microscopy (SEM) analysis of the grey colony variants that arose at both temperatures. This study further highlights the importance of routine whole-genome sequencing when studying phenotypic traits of *L. monocytogenes* isolates.

RESULTS

IVEE performed at 42°C and 30°C promotes the emergence of grey-colored colonies. In our previous study, we demonstrated that *L. monocytogenes* strains with *sigB* mutant genotypes and phenotypes exhibit increased growth rate and competitive advantage when grown in brain heart infusion (BHI) at 42°C but not at 30°C (21). In this study, we sought to investigate the impact of incubation temperatures on the spontaneous emergence of alleles within the *sigB* operon. The previously identified σ^B-dependent grey colony coloration phenotype was used to distinguish potential *sigB* mutant colonies from wild type (WT) (Fig. 1C) (21). Grey-colored colonies were detected from passage 15 at a relative abundance of 0.39% within the population and progressively increased to ~21% relative abundance in the following passages (Fig. 1A). Interestingly, grey-colored colonies were also detected in the IVEE performed at 30°C. These variants emerged from passage 10 from an initial relative abundance of ~0.1% and increased to ~1% until the end of the experiment (Fig. 1B).

Mutations arise in the *sigB* operon at 42°C and in *agrCA* at 30°C. To identify genotype(s) responsible for the grey colony coloration observed from IVEE, we obtained whole-genome sequences (WGS) from 14 colonies isolated from the IVEE performed at 42°C (9 grey and 5 white) and 10 colonies isolated from the IVEE performed at 30°C (6 grey and 4 white). We verified that all of the analyzed grey-colored colonies isolated at 42°C carried a single nucleotide polymorphism (SNP) in an open reading frame (ORF) coding one of the positive regulators of σ^B (*rsbS*, *rsbT*, and *rsbU*) or in *sigB* itself (Table 1). Additionally, one isolate (designated variant 77) harbored a 32-bp deletion in *rsbU*. As previously observed (21), all SNPs produced either frameshifts or nonsense mutations, which caused truncations of the corresponding proteins. In contrast, all grey variants isolated from the IVEE performed at 30°C carried either insertions or deletions (indels) or SNPs in the ORFs of *agrC* or *agrA*. Additionally, none of the isolated white-colored colonies at either temperature harbored mutations in either the *sigB* or *agrCA* operons. To assess the influence of the Agr system on the colony coloration phenotype, the wild-type and the isogenic Δ*agrA* strains were grown separately at 30°C overnight and mixed in a ratio of 1:1 and plated in BHI agar plates at a final concentration of ~10^2 CFU · mL^{-1}. These results verified that loss of the Agr system, similarly to σ^B, is responsible for the grey colony phenotype observed during the IVEE performed at 30°C (Fig. 1D).

Acid-sensitive grey-colored colonies were only isolated at 42°C. In our previous study, we reported that the loss of σ^B-positive regulator genes (*rsbS*, *rsbU*, and *rsbV*) results in an increase in acid sensitivity (21). Several of the grey-colored colonies obtained during the IVEE were challenged under lethal acidic conditions (BHI acidified

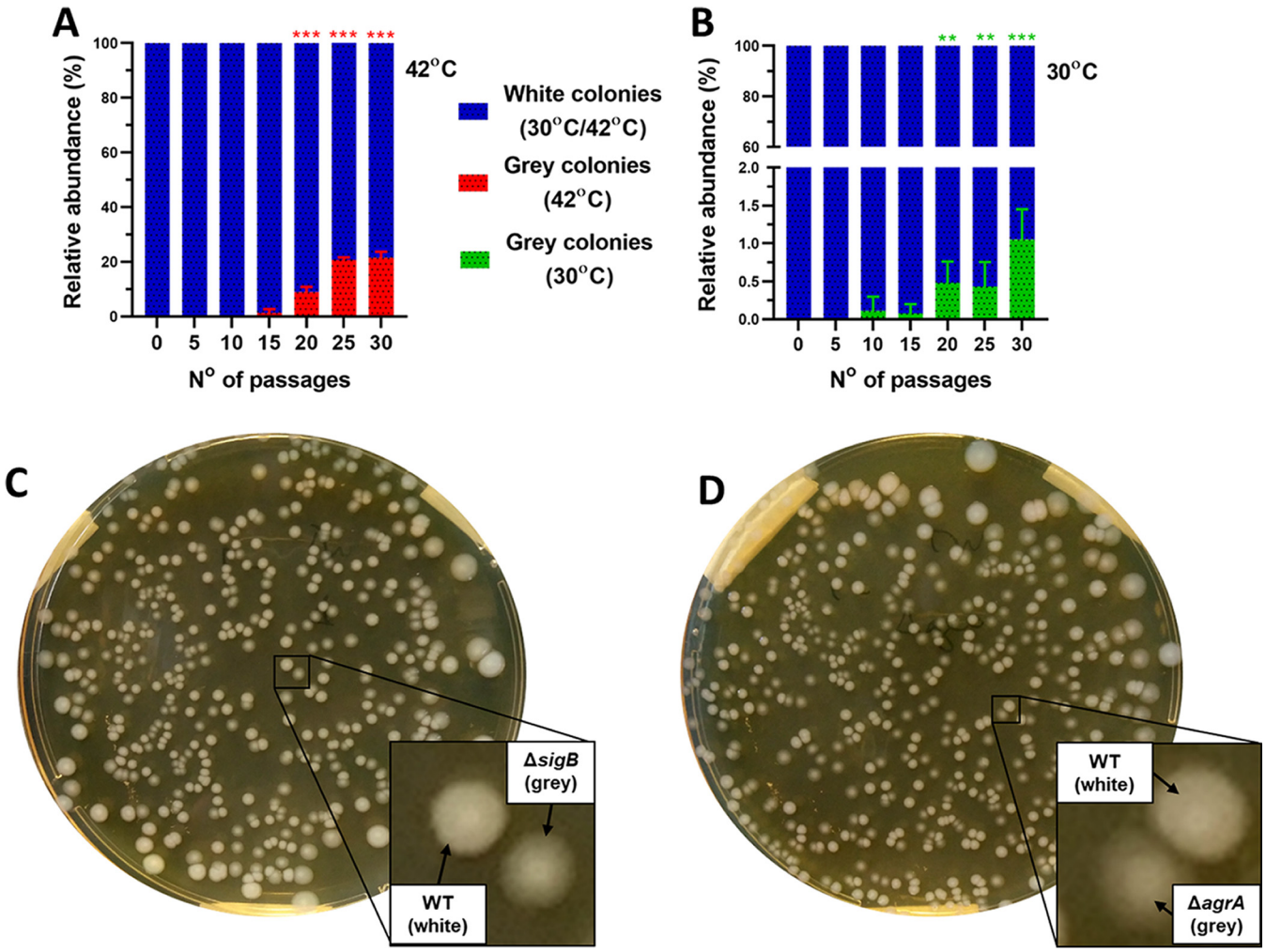

FIG 1 Differential emergence of grey colony phenotypic variants during *in vitro* evolution experiments at 42°C and 30°C. *In vitro* evolution experiments where cultures of *L. monocytogenes* EGD-e wild-type strain were grown in BHI at either 42°C (A) or 30°C (B) overnight. Passages were made every 24 h for a total of 30 days by diluting the cultures in a 1:100 ratio into fresh BHI. Every 5 days, the number of white and grey colonies was used to calculate the percentage of relative abundance. Panels C and D show that the colony coloration between the whiter WT and the greyish Δ*sigB* (C) and Δ*agrA* (D) strains in BHI agar plates were incubated at 37°C for 24 h and a further 6 days at 30°C. At least two independent biological replicates were performed for each incubation temperature. Statistical analysis was performed using a paired Student's *t* test relative to passage 0 (**, *P* value of $<$0.01; ***, *P* value of $<$0.001).

to pH 2.5 at 37°C) along with a few selected white-colored colonies isolated during the IVEE. The parental strain and white colonies exhibited similar acid tolerance, reflected by a similar pattern of survival after 30 min in pH 2.5 at 37°C (Fig. 2A). In contrast, the Δ*sigB* mutant strain and grey-colored colonies isolated at 42°C showed an approximately 3 Log_{10} ($CFU.ml^{-1}$) reduction after 30 min at pH 2.5 (Fig. 2A). At the same time, the Δ*agrA* mutant strain exhibited a small, although not significant (0.4705 Log_{10}; $P = 0.3445$), reduction in resistance, while none of the grey colonies isolated at 30°C showed a reduction in acid resistance comparable to the Δ*sigB* mutant (Fig. 2B).

Confirmation of loss-of-function alleles in the *sigB* operon and *agrCA* ORFs. The impact of the identified alleles on the activity of σ^B was assessed by transforming several colonies with vector pKSV7-$P_{lmo2230}$::*egfp*, which harbors a σ^B-dependent reporter (30). The σ^B activity was determined through the quantification of enhanced green fluorescent protein (eGFP) expression in the reporter strains. Reduced σ^B activity was confirmed in grey-colored colonies isolated at 42°C, which harbor *sigB* alleles (Fig. 3A), while the grey colonies isolated at 30°C, harboring alleles at the *agrCA* genes, retained similar σ^B activity compared with that of the parental strain (Fig. 3A).

Strains transformed with pGID310-P_{agrB}::*gfp*::*bgaB*, the Agr reporter plasmid, and with an intact Agr system formed blue colonies in BHI agar supplemented with X-Gal

TABLE 1 List of strains obtained during the *in vitro* evolution experiments performed at 42°C and 30°C and their respective results obtained from WGS

Strain code	Isolation temp (°C)	No. of biological replicates	No. of passages	Colony coloration	Acid resistance[a]	Biofilm formation[e]	Allele location[b]		Allele result[c]
							in *sigB* operon	In *agr* operon	
1[h]	42	1	5	Grey	Sensitive		Δ(*rsbT*) 89 (−G)		p.G30Afs*15
4[h]	42	1	5	White	Resistant				
18	42	1	10	Grey	Sensitive		Δ(*sigB*) 280 (−A)		p.I94Sfs*19
32	42	1	20	Grey	Sensitive		Δ(*rsbT*) 89 (−G)		p.G30Afs*15
33	42	1	20	White	Resistant				
50	42	2	10	White	Resistant				
51[h]	42	2	15	Grey	Sensitive		*rsbU* CAA→TAA (codon 317)		Q317*
58[h]	42	2	20	Grey	Sensitive		*rsbS* GTG→GTA (codon 1)[d]		M1V[d]
60	42	3	20	Grey	Sensitive		IN(*rsbT*) 52 (+G)		p.A18Gfs*4
65[h]	42	3	20	White	Resistant				
66[h]	42	3	25	Grey	Sensitive		IN(*rsbT*) 52 (+G)		p.A18Gfs*4
70	42	3	25	White	Resistant				
74	42	3	30	Grey	Sensitive		IN(*rsbU*) 316 (+A)		p.T108Nfs*10
77	42	3	30	Grey	Sensitive		Δ(*rsbU*) 912 (−32 bp)		K304*
36[h,i]	30	1	10	Grey		−		*agrA* GGT→GAT (codon 84)	G84D
37[h,i]	30	1	10	White		+			
38	30	1	10	Grey		−		IN (*agrC*) 460 (+T)	p.S156Ffs*22
89	30	2	15	White		+			
90[h,i]	30	2	20	Grey		−		*agrC* CAG→TAG (codon 224)	Q224*
92[h,i]	30	2	20	Grey		−		*agrC* GGC→GGT (codon 399)	G399C
93[h,i]	30	2	20	White		+			
95[h,i]	30	3	20	Grey		−		*agrC* Δ21 bp (at 1,165–1,296 bp)	[f]
96	30	3	20	White		+			
99[h,i]	30	3	25	Grey		−		IN (*agrC*) 764 (+TGATAATAA)	[g]

[a]Acid tolerance phenotype shown in Fig. 2A.
[b]SNP location in *L. monocytogenes* EGD-e chromosome identified by WGS.
[c]Nomenclature adapted from that recommended by the Human Genome Variations Society (59).
[d]GTG codon consists of an alternative start codon in *L. monocytogenes*.
[e]Biofilm formation results (see Fig. S3 in the supplemental material).
[f]In frame knockout of the ATP lid in the HATPase domain (no frameshift or SNP identified).
[g]In frame insertion, sequence duplication (+TGATAATAA) between the coiled coil and HATPase domains (no frameshift or SNP identified).
[h]Strains transformed with pKSV7-$P_{lmo2230}$::*egfp*.
[i]Strains transformed with pGID310-P_{agrB}::*gfp*::*bgaB*.

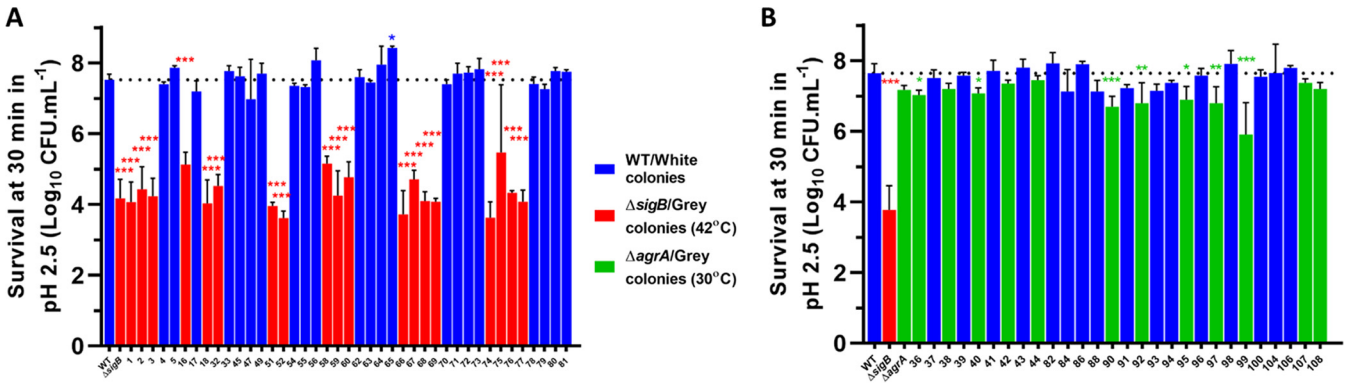

FIG 2 Grey colonies isolated from *in vitro* evolution experiments at 42°C have acid-sensitive phenotypes. Cultures of *L. monocytogenes* EGD-e wild-type, Δ*sigB*, and Δ*agrA* strains and white and grey colonies isolated from the *in vitro* evolution experiments at 42°C (A) and 30°C (B) were grown overnight in BHI at 37°C. Cultures were challenged in acidified BHI medium (pH 2.5) at 37°C. Samples were taken at 0 and 30 min for viable counts. Blue bars represent white colony strains, while red bars represent the Δ*sigB* strain or grey colonies isolated at 42°C and green bars represent the Δ*agrA* strain or grey colonies isolated at 30°C. Two independent biological replicates were made. Statistical analysis was performed using a paired Student's *t* test by comparing with the parental strain (*, *P* value of <0.05; **, *P* value of <0.01; ***, *P* value of <0.001).

(5-bromo-4-chloro-3-indolyl-β-D-galactopyranoside). Reporter strains carrying *agrCA* mutations and Δ*agrA* formed white colonies in contrast to the blue colonies formed by the parental strain (Fig. 3B to D). Interestingly, the isogenic Δ*sigB* mutant exhibited a slightly bluer coloration compared with that of the parental strain at all temperatures. In addition, a slight increase of *agrB* transcripts (0.95 $\log_2$; $P = 0.015$), a highly Agr-de-

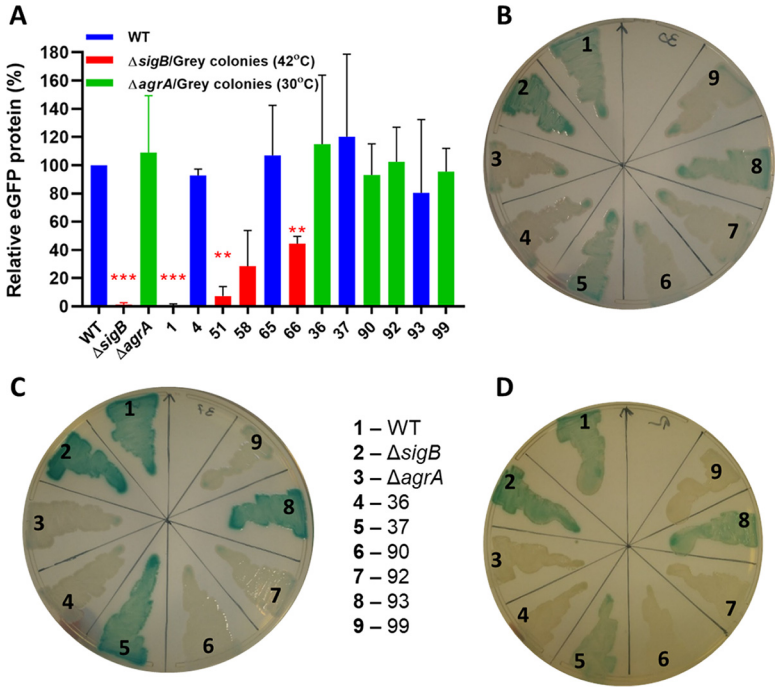

FIG 3 Strains carrying alleles in *sigB* or *agr* operons exhibit reduced activity in each of the respective systems. Stationary-phase cultures of WT, Δ*sigB*, and Δ*agrA* strains and colonies isolated from the *in vitro* evolution experiments at both temperatures were transformed with pKSV7-$P_{lmo2230}$::*egfp* (A) and pGID310-P_{agrB}::*gfp*::*bgaB* (B, C, D). (A) Percentage of eGFP signal normalized relative to the WT. Quantification was obtained from Western blot images. Blue bars represent eGFP levels from the wild-type strain or white-colored colonies, red bars represent levels in the Δ*sigB* strain and grey-colored colonies isolated at 42°C, and green bars represent levels in the Δ*agrA* strain and grey-colored colonies isolated at 30°C. Cultures transformed with pGID310-P_{agrB}::*gfp*::*bgaB* were patched in BHI agar plates, supplemented with Chl and X-Gal, and incubated at 30°C (B), 37°C (C), and 42°C (D) for 48 h. For strain details, refer to Table 1. Western blot quantification was generated from two independent biological replicates. Statistical analysis was performed by a paired Student's *t* test (**, *P* value of <0.01; ***, *P* value of <0.001).

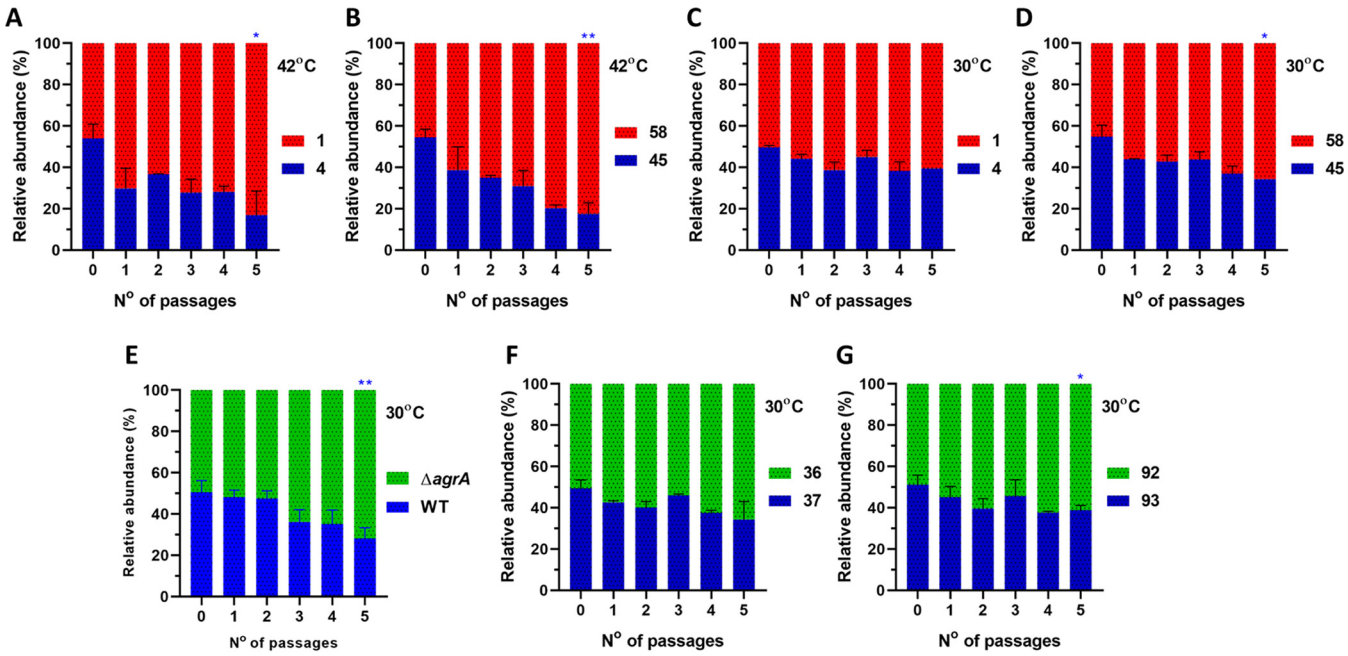

FIG 4 Strains carrying *sigB* or *agr* alleles exhibit a competitive advantage during mixed culture passaging. Competition experiments were performed with white versus grey colonies (starting ratio 1:1) isolated during the *in vitro* evolution experiments. Mixed cultures were passaged at 42°C (A, B) or 30°C (C, D, E, F, G). Blue bars represent the parental strain and white-colored colonies, while red and green bars represent the *sigB* and *agr* mutants, respectively. Data were generated from two independent biological replicates. For strain details, refer to Table 1. Statistical analysis was performed using a paired Student's *t* test (*, *P* value of <0.05; **, *P* value of <0.01).

pendent gene, was observed in the Δ*sigB* strain (see Fig. S1 in the supplemental material). These results suggest that σ^B exerts a repressive effect on the Agr system, an effect similar to that observed in *Staphylococcus aureus* (31). Finally, we observed that the activity of both reporter systems was unchanged in all of the tested white colonies.

***agr* mutant strains exhibit a small competitive advantage against the parental strain.** In our previous study, we found that *sigB* mutant strains exhibit increased competitive advantage at 42°C but not at 30°C when competing with the parental strain (21). In our competition experiments, we verified that *sigB* mutant strains exhibit a similar advantage over the parental and *sigB*$^+$ strains at 42°C (Fig. 4A and B; see also Fig. S2A and B in the supplemental material), and as expected, this phenotype was abolished at 30°C (Fig. 4C and D; see also Fig. S2C and D), which is in agreement with our previous observations (21). The impact of the *agrCA* alleles was also assessed at 30°C by competing the parental strain against the isogenic Δ*agrA* strain. The results revealed a small competitive advantage that allowed the Δ*agrA* strain to reach 71.77% ($P = 0.0066$) of the total population after five passages at 30°C (Fig. 4E). Competitions between the obtained *agr* mutant strains (colonies 36 and 92) were tested against their *agr*$^+$ counterparts (colonies 37 and 93). A comparatively small competitive advantage in the *agr* mutant strains relative to the *agr*$^+$ strains was observed after 5 passages (65.7% and 61.12%) (Fig. 4F and G, respectively). However, the *agr* mutant 36 strain could not outcompete the parental strain (Fig. S2E), while the *agr*$^+$ 37 strain was overtaken by the Δ*agrA* mutant strain (Fig. S2F).

We also aimed to identify the origin of this competitive behavior conferred by the *agrCA* alleles by measuring the growth rates of several *agr*$^+$ and *agr* mutant isolates at 30°C. However, the results showed no observable growth changes under these conditions (Fig. S2G and H). In *L. monocytogenes*, Agr activity has been linked with cell surface attachment and biofilm formation (26, 27, 32, 33); therefore, we further tested the impact of the Agr loss-of-function alleles on the biofilm formation. The results revealed a significant reduction in biofilm formation in Δ*agrA* and *agr* mutant strains compared with those of the parental and *agr*$^+$ strains (see Fig. S3 in the supplemental material).

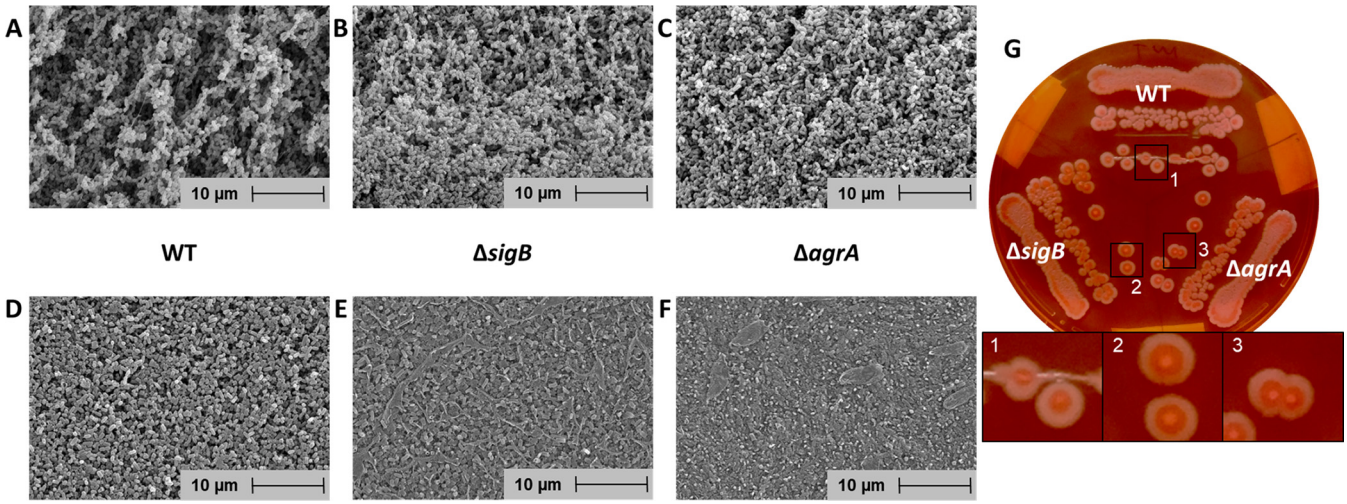

FIG 5 Colony architecture is influenced by either Δ*sigB* or Δ*agrA* deletions. Images recorded by scanning electron microscopy of 7-day-old colonies of wild type (A, D), Δ*sigB* (B, E), and Δ*agrA* (C, F) strains grown in BHI agar plates at 30°C. Under these conditions, the grey colony phenotype was evident in the mutant strains. Images correspond to the colony border (A, B, C) or center (D, E, F). (G) Colonies of *L. monocytogenes* EGD-e WT, Δ*sigB*, and Δ*agrA* strains grown in BHI agar supplemented with Congo red (25 μg · mL^{-1}). Plates of Congo red were incubated for 24 h at 37°C and for three more days at 30°C. Representative data from three biological replicates are shown.

Δ*sigB* and Δ*agrA* deletions influence the colony architecture. We hypothesize that the colony coloration differences between the parental strain and the remaining variants are a direct result of differences in the opacity of their colonies (i.e., colonies formed by the wild type were more opaque compared to those formed by *sigB* mutants and *agr* mutants). Here, 7-day-old colonies of *L. monocytogenes* EGD-e wild-type, Δ*sigB*, and Δ*agrA* strains were prepared and observed through SEM. The SEM images revealed irregular structures formed by cell aggregates at the borders of the wild-type colonies (Fig. 5A), while the Δ*sigB* and Δ*agrA* mutant strains exhibited much less pronounced structures (Fig. 5B and C). Similar irregular structures were also observed while using different incubation conditions in a different study (34). At the center of the colonies, however, the wild-type strain displayed discernible cells with a well-defined rod-like shape (Fig. 5D), while cells of both Δ*sigB* and Δ*agrA* mutant strains were embedded within an extracellular matrix (Fig. 5E and F). Additionally, when grown in BHI supplemented with Congo red, both mutant strains exhibited a redder coloration than the wild-type strain (Fig. 5G).

***agrCA* alleles show high PMSC rates similar to the positive regulators of σ^B.** The spontaneous emergence of *agrCA* alleles in the IVEE performed at 30°C prompted us to investigate if *agrCA* alleles also occur among wild isolate strains of *L. monocytogenes*. For this, we employed the previously described approach for analyzing premature stop codon (PMSC) rates (21) to survey 40,080 *L. monocytogenes* genomes publicly available on the NCBI database. We examined the PMSC occurrence rate (per 100 bp) in the *agr* operon compared to genes from several other gene categories, including two-component systems, the *sigB* operon, genes used for multilocus sequence type (MLST) analysis, metabolic genes, and virulence genes (Fig. 6). As expected, results for the *sigB* operon and other genes used as controls (MLST genes, sigma factors and metabolic genes, *rsbR1* paralogues, virulence genes) were similar to our earlier observations. The PMSC rate for *agrC* was comparable to the highest observed in the *sigB* operon and was substantially higher in the case of *agrA* (Fig. 6). In clear contrast, PMSCs in all other two-component systems encoding genes were very rare, with *resD* as the sole exception. ResD is known to be important for mediating carbohydrate-based repression on virulence genes as well as controlling respiration in *L. monocytogenes* (35). More interestingly, the high PMSC rates were restricted to *agrCA*, in contrast with the extremely low rates of *agrBD*. Taken together, these results indicate a high incidence of *agrCA* loss-of-function alleles among field isolates.

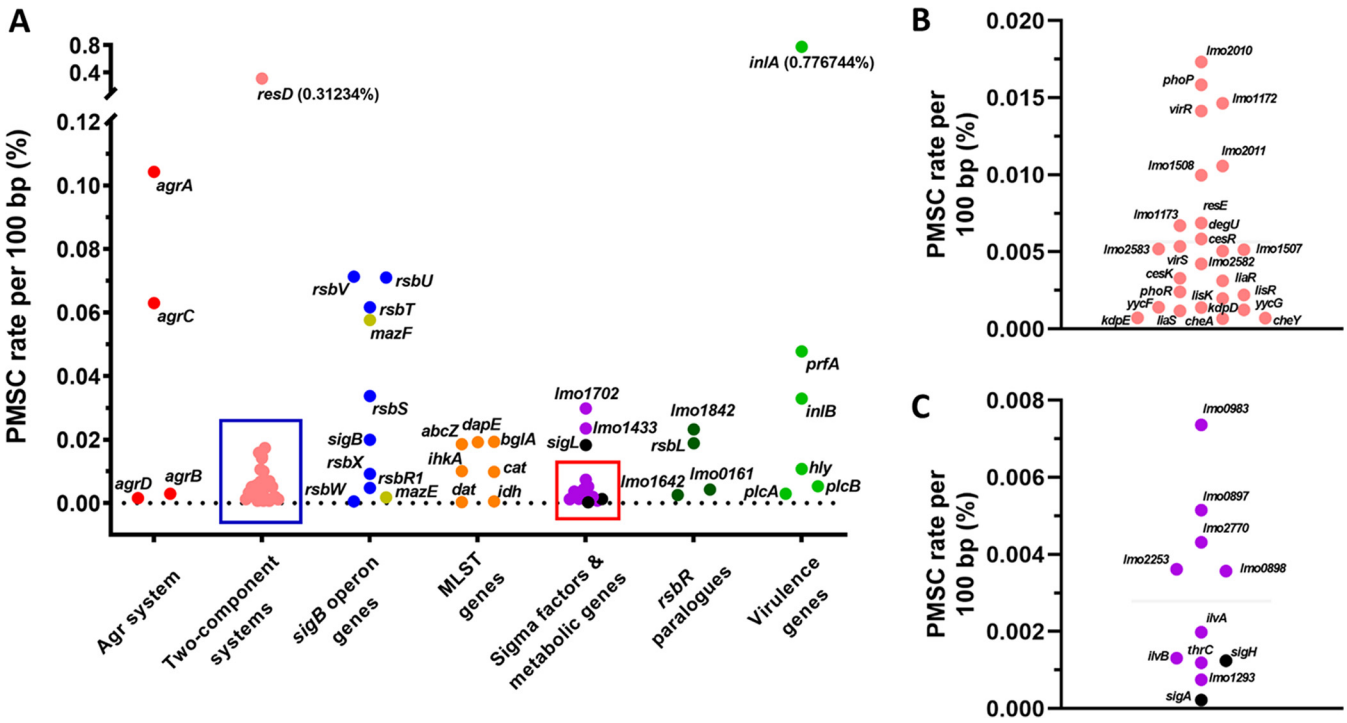

FIG 6 High frequency of PMSCs detected in the *agrCA* and *sigB* operons. *In silico* analysis of 40,080 genomes of *L. monocytogenes* strains publicly available. (A, B, and C) PMSC rate normalized by 100 bp of the open reading frame length for genes comprising the *agr* operon (red), two-component systems (pink), *sigB* operon (blue), *mazEF* (yellow), MLST genes (orange), sigma factors (black), metabolic genes (purple), rsbR1 paralogues (dark green), and virulence genes (light green). (B and C) Expanded area indicated by the blue and red squares in panel A, respectively.

Measurements of the Agr activity in the strain collections. Since the *in silico* analysis revealed the prevalence of PMSC mutations affecting *agrC* and *agrA*, AgrC and AgrA, we sought to investigate whether such mutations can influence the activity of the Agr system. An existing laboratory strain collection of 168 *L. monocytogenes* strains with WGS available (36) was screened for *agr* operon mutations giving rise to PMSCs. Five strains in this collection were found to carry PMSCs in the *agrCA* genes (Table 2). The well-studied laboratory reference 10403S harbors an *agrA* mutation predicted to truncate AgrA. The clinical isolate MQ140031 bears an in-frame deletion of 141 amino acids in *agrA*. Strains 1389, 1384, and 1378 carry *agrC* alleles, and these are among 25 strains recommended for assessing food challenge studies by the European Union Reference Laboratory of *L. monocytogenes*. A truncation in the 5′-end region of *agrC* rendered the majority of the protein untranslated in strain 1389; a transposon sequence insertion in the 3′-end region of *agrC* disrupted its translation in strain 1384; a frameshift at the stop codon resulted in a longer version of *agrC* that overlaps *agrA*

TABLE 2 List of *L. monocytogenes* isolates that carry PMSC in *agr* operon genes and their respective reference strains that carry intact *agr* operon genes

Strain code	Lineage	CC[a]	Allele location in *agr* operon	Allele result
1389	II	31	*agrC* TCA→TAA (codon 27)	S27*
1371	II	31		
10403S	II	7	Δ(*agrA*) 628 (−A)	p.N221Ifs*3
1445	II	7		
1384	I	59	(*agrC*) IN at 1106 bp[b]	p.F370Vfs*10[b]
3447	I	59		
1378	I	5	Δ(*agrC*) 1286 (−A)	p.I430Lfs*25
1441	I	5		
MQ140031	I	1	Δ(*agrA*) 60 (−426 bp)	D23_E164del
MQ130032	I	1		

[a]CC, clonal complex.
[b]Frameshift caused by transposon insertion at the 5′ end of *agrC*.

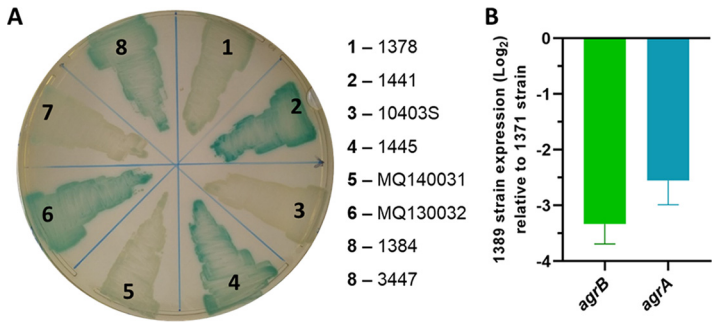

FIG 7 Field isolates carrying alleles in the *agr* operon exhibit reduced activity in each of the respective systems. (A) Isolates that integrated pGID310-P_{agrB}::*gfp*::*bgaB* were patched in BHI agar plates supplemented with Chl and X-Gal and incubated at 37°C for 48 h. (B) Expression of *agrB* and *agrA* in strain 1389 grown to stationary phase (16 h) at 37°C was compared to strain 1371 by RT-qPCR experiment.

open reading frame in strain 1378. As these strains were from different genetic backgrounds, a control strain from the same clonal complex (CC) was selected for each to assess the impact of these mutations on the Agr activity. For this, eight strains were transformed with pGID310-P_{agrB}::*gfp*::*bgaB*, and the reporter plasmid was integrated into their genomes. Agr activities were visualized on medium containing X-Gal, and Agr activity was determined by reverse transcriptase quantitative PCR (RT-qPCR) analysis of the transcription of *agrB* and *agrA*. In both assays, the Agr activity was reduced in all strains carrying either *agrC* or *agrA* alleles (Fig. 7A and B).

DISCUSSION

In this study, we investigated the conditions leading to the emergence and proliferation of variants harboring alleles within the *sigB* operon in *L. monocytogenes*. We set up IVEEs at either 42°C or 30°C, and variants forming greyish, more translucent colonies were detected at both temperatures (Fig. 1A and B). Grey variants isolated from the IVEE performed at 42°C harbored loss-of-function alleles at the *sigB* operon (Table 1) and exhibited reduced acid tolerance and decreased σ^B activity (Fig. 2A and Fig. 3A). However, grey variants isolated from the IVEE performed at 30°C carried loss-of-function alleles in *agrCA* genes (Table 1; Fig. 3B to D). In both cases, grey variants were able to outcompete the parental strain at the respective temperatures, although this effect was more apparent for the *sigB* operon mutants (Fig. 4A to G). Additionally, we analyzed all publicly available genomes of *L. monocytogenes* and identified high rates of PMSC occurrence in both the *sigB* operon and *agrCA* ORFs (Fig. 6A).

In several other studies, loss-of-function alleles within the *sigB* operon were identified in newly constructed mutant strains or strains isolated from intragastrically inoculated mice (21, 37–39), suggesting that such alleles can emerge spontaneously in laboratory-grown cultures. Indeed, we observed the spontaneous emergence of strains harboring *sigB* alleles in our IVEE at 42°C; however, the parental strain still accounted for ~80% of the population at the end of the experiment (Fig. 1A). It is known that alleles conferring increased fitness can coexist with the parental strain for up to ~10,000 generations until additional mutations further increase the mutant's fitness (reviewed in reference 40). However, only ~200 generations occurred during the 30-day span of our experiment. We hypothesize that *sigB* mutants still require additional fitness conferring mutations before being able to fully overtake the parental strain population. While 42°C conferred increased competitive fitness to *sigB* mutants (Fig. 4A and B; see also Fig. S2A and B in the supplemental material) (21), this advantage was abolished at 30°C (Fig. 4C and D; see also Fig. S2C and D). These observations probably explain the apparent absence of *sigB* mutants in the IVEE performed at 30°C (Table 1). It is known that σ^B is triggered during temperature upshift (to 45 to 48°C) in *L. monocytogenes* (41, 42). Moreover, under mild stresses, the σ^B activity is known to hinder the growth rate of *L. monocytogenes* (18, 21). We hypothesize that the competitive

disadvantage observed at 42°C for the wild type is a consequence of a higher activation of σ^B, resulting in a slower growth rate. Interestingly, similar mutations in the gene encoding the alternative sigma factor σ^S (*rpoS*), a homologue of σ^B in Gram-negative bacteria, are frequently found in laboratory-grown *Escherichia coli* and *Pseudomonas aeruginosa* (43, 44).

The exact mechanism responsible for the growth suppression generated by the activation of σ^B is still unclear, but a few hypotheses have been suggested (7, 21). First, competition between the housekeeping sigma factors A (σ^A) and σ^B for the RNA polymerase may direct transcription away from genes with growth-related functions. Similarly, an increase in mRNA concentration from genes belonging to the general stress response regulon will require a significant fraction of the cellular ribosome pool, thereby limiting the potential to translate housekeeping mRNA. Secondly, redirection of resources and energy from growth to survival mechanisms might negatively impact growth. Thirdly, it is possible that deliberate suppression of growth through a σ^B-dependent mechanism might occur as has been suggested for the σ^B-dependent small RNA (sRNA) Rli47 (45). In this scenario, the biological rationale is that reduced growth might increase the likelihood of survival, since it allows time for homeostatic and repair mechanisms to function. Finally, if σ^B plays a role in producing secreted enzymes or molecules that can be shared within the population, mutants could arise as cheaters within the population that take advantage by exploiting the availability of "public" resources. Further experimental work will be needed to investigate which of these explanations is driving the selective pressure for σ^B loss-of-function mutants to emerge at 42°C.

The IVEE performed at 30°C revealed grey variants harboring alleles in the ORF of either *agrC* or *agrA* instead of PMSC in the *sigB* operon (Fig. 1; Table 1), which lead to the inactivation of the Agr system (Fig. 3B to D). Additionally, the *agr* mutant alleles seem to provide a small competitive fitness advantage at 30°C (Fig. 4E to G); however, the growth rates of these variants remained unchanged (Fig. S2G and H). Interestingly, the *agr* mutant alleles impaired the biofilm formation in conical-bottomed 50-mL plastic tubes under shaking conditions (see Fig. S3 in the supplemental material). The Agr system plays a critical role in the surface cell attachment during the initial stages of the biofilm formation (27). We speculate that a small fraction of the parental strain cells attaches and forms biofilm on the wall of the flask, while the emerging *agr* mutant cells, unable to attach to the flasks surfaces, are left in the planktonic phase. This phenotype could contribute to a disproportional ratio of parental/*agr* mutant that is magnified with the successive passages. Interestingly, while the Agr activity is crucial for the biofilm formation at low temperatures, this phenotype is reverted at 37°C (25), which may explain the absence of Agr alleles detected in the IVEE performed at 42°C. Alternatively, other nonexclusive factors may contribute to the emergence of *agr* mutations, as the Agr and other QS systems represent an energetic burden and are detrimental for growth in certain environments (46–48). In a recent study, the *L. monocytogenes* Agr system was found to downregulate genes involved in the synthesis of *S*-adenosylmethionine in nutrient-poor media (25, 49), suggesting that Agr represses metabolism under specific conditions.

The high frequencies of PMSC in *agrCA* genes among publicly available *L. monocytogenes* genome sequences contrast with the extremely low frequency of PMSC found in *agrBD* genes (Fig. 6). In accordance with this, only *agrCA* alleles emerged during the *in vitro* evolution experiment at 30°C. The *agrCA* mutants may behave as social cheaters, which still contribute to the extracellular autoinducing peptide (AIP) pool and stimulate the Agr activity on *agr*$^+$ strains. However, these strains do not bear the energetic burden of contributing to the community. To our knowledge, the contribution of the Agr system in the production of public goods in *L. monocytogenes* communities is currently uncharacterized. Our data suggest that similarly to σ^B, the deployment of the Agr system possesses a fitness tradeoff for *L. monocytogenes* under specific conditions.

In our previous study, we found that Δ*sigB* and *sigB* mutant strains formed greyish and more translucent colonies compared with those of the parental strain (21). Here, we found that Δ*agrA* and *agr* mutant strains form similar colonies to those of *sigB*

mutants (Fig. 1D). Previous studies found that σ^B is responsible for the cell wall thickness in response to blue light stress, which in turn impacts the colony opaqueness (20, 50). Interestingly, the Agr system also regulates the expression of proteins participating in the cell wall peptidoglycan biosynthesis in *L. monocytogenes* (49). It is plausible that the colony coloration disparities observed in this study are a consequence of differences in cell envelope composition; however, future studies will have to confirm this hypothesis.

SEM revealed complex multicellular structures close to the colony edges of the parental colonies (Fig. 5A), while cells at the center were compact and well defined (Fig. 5D). These structures were less evident in both Δ*sigB* and Δ*agrA* strains (Fig. 5B and C), while their colony centers apparently had a more abundant extracellular matrix (Fig. 5E and F), which seems correlated with the red coloration observed in plates supplemented with Congo red (Fig. 5G). *S. aureus* is known to form irregular biofilms that are dependent on the production of the Agr-dependent phenol-soluble modulins (PSM) (51); however, PSM have not been identified in *L. monocytogenes*. It is not surprising that both σ^B and Agr regulate biofilm formation, as previous studies demonstrated an overlap in their regulons (25, 26); however, the environmental signals and genes responsible for these phenotypes are currently unknown.

In summary, our results further suggest that laboratory conditions could inadvertently select unwanted secondary mutations in nonessential or energetic expensive systems. These findings highlight the need for caution in the routine culturing of laboratory stocks of *L. monocytogenes*, especially during the execution of mutagenesis protocols that require an elevated temperature incubation, to avoid inadvertently picking up a mutation in one of these systems. Such mutations could easily confound any phenotypic study of this pathogen, potentially leading to erroneous conclusions. It seems appropriate, therefore, to suggest that whole-genome sequencing should be implemented as a standard verification protocol for any newly constructed mutants to avoid misinterpretation of phenotypical data.

MATERIALS AND METHODS

Bacterial strains, plasmids, and primers. *L. monocytogenes* and *E. coli* strain plasmids and primers used in this study are shown in Table 3. Strains were grown in brain heart infusion (BHI) broth or agar (Lab M) at 37°C with constant shaking of 150 rpm unless otherwise specified. Cells were grown overnight for 16 h to reach the stationary phase. Antibiotics were added to the growing media when required at the following concentrations: ampicillin (Amp) at 100 μg · mL^{-1} for the *E. coli* strain and chloramphenicol (Chl) at 10 μg · mL^{-1} and tetracycline (Tet) at 2.5 μg · mL^{-1} for *L. monocytogenes* strains.

Long-term incubation *in vitro* evolution setup. The *L. monocytogenes* EGD-e wild-type strain was grown overnight at either 30°C or 42°C in 50-mL conical bottom flasks containing 5 mL of fresh BHI with a constant shaking at 150 rpm. Each overnight culture was subcultured into two flasks through a dilution of 1:100 and allowed to grow for 24 h at the respective temperatures. Passages consisting of a 1:100 dilution of each culture into fresh BHI was made every 24 h for 30 days. Sampling was made every five passages by serial diluting in phosphate-buffered saline (PBS) (Sigma) to 10^{-7} and plating in BHI agar plates. Plates were incubated at 37°C for 24 h and a further 6 days at 30°C. Colony coloration was registered, and relative abundance was calculated as the percentage of the total number of colonies. The white/grey colony colorations differentiated the nonmutated parental strain from strains carrying putative alleles in the *sigB* and *agr* operons. This discerning method was validated in our previous study (21). Counts were performed with the naked eye using a black background. A total of six flasks, two per biological replicate, were used at each temperature.

Congo red agar plates. Cultures of *L. monocytogenes* WT, Δ*sigB*, and Δ*agrA* strains were separately grown in BHI overnight at 30°C. Cultures were serially diluted in PBS (Sigma) until 10^{-7}, and 10 μL of the dilutions between 10^{-5} and 10^{-7} were plated in BHI agar plates supplemented with Congo red (Sigma) at a final concentration of 25 μg · mL^{-1}. Plates were incubated for 24 h at 37°C and transferred to 30°C for three more days until the differentiation in colony coloration was observable.

Acid tolerance in BHI at pH 2.5. Stationary-phase cultures of the wild-type, Δ*sigB*, Δ*agrA*, and mutant strains were centrifuged at 14,000 rpm for 1 min and resuspended in BHI medium previously acidified with 5 M HCl to pH 2.5. Resuspensions were incubated in a water bath at 37°C for 30 min. Samples were taken at 0 and 30 min, serially diluted from 10^{-7} to 10^{-2} in PBS (Sigma) and plated onto BHI agar plates. Plates were incubated at 37°C, and colonies were counted 24 h afterwards. Two biological replicates were made.

Whole-genome sequencing. The genomic DNA (gDNA) of strains obtained during the IVEE at both temperatures was extracted with DNeasy blood and tissue kit (Qiagen) according to the manufacturer's

TABLE 3 List of *L. monocytogenes* strains, plasmids, and primers used in this study

Strain, plasmid, or primer	Primer name	Reference/source
Strain		
Escherichia coli One Shot TOP10		Invitrogen
Listeria monocytogenes EGD-e (wild type)[a,b]		Gift from K. Boor (Cornell)
L. monocytogenes EGD-e; Δ*sigB*[a,b]		21
L. monocytogenes EGD-e; Δ*agrA*[a,b]		33
L. monocytogenes 1378[b]		60
L. monocytogenes 1441[b]		60
L. monocytogenes 10403S[b]		Gift from K. Boor (Cornell)
L. monocytogenes 1445[b]		60
L. monocytogenes MQ140031[b]		61
L. monocytogenes MQ130032[b]		61
L. monocytogenes 1384[b]		60
L. monocytogenes 3447[b]		60
L. monocytogenes 1389		60
L. monocytogenes 1371		60
Plasmid		
pKSV7-P$_{lmo2230}$::*egfp*		30
pGID128-P$_{argB}$::*gfp*		27
pDL		53
pGID310-P$_{agrB}$::*gfp*::*bgaB*		This study
Primers (5′ to 3′)		
GCCTTGTCGCCATCTTTG		*egfp_lmo2230*_F
GGCCGTTTACATCTCCATC		*egfp/bgaB_lmo2230*_R
AAATGGAAAAGCCAACTGTGA		*bgaB_agrB*_F
CGAGATCTAGCTAGGAGGTATAATCATGAATGTGTT		*bga11*
AAAGATCTGAACGAGACTTCTCTAAACCTTC		*bga12*
TGGGGAGCAAACAGGATTAG		16S_RT_F
TAAGGTTCTTCGCGTTGCTT		16S_RT_R
CATATTCGAAGTGCCATTGC		*lmo2230*_F
CTGAACTAGGTGAATAAGACAAAC		*lmo2230*_R
GCGAATGGTATTAGCAACGC		*agrB*_F
GCTTGCGCCATTTGTTTTTC		*agrB*_R
GAAGAAGGTTTCTCTACAAAAGGAG		*agrA*_UNI_RT_F
GTTAACCTTTCTCGCTGCATT		*agrA*_UNI_RT_R
GCTTGCGCCATTTGTTTTTC		*agrB*_UNI_RT_F
GCGAATGGTATTAGCAACGC		*agrB*_UNI_RT_R

[a]Strains later transformed with the σ^B reporter plasmid pKSV7-P$_{lmo2230}$::*egfp*.
[b]Strains later transformed with the Agr reporter plasmid pGID310-P$_{agrB}$::*gfp*::*bgaB*.

recommendations. Purified gDNA was sent to MicrobesNG for WGS, and the retrieved trimmed reads were used for SNP analysis performed in Breseq (52). The chromosomal sequence of *L. monocytogenes* EGD-e (NCBI RefSeq accession number NC_003210) was used as the reference genome.

Construction of the *agr* system reporter pGID310 (P$_{agrB}$::*gfp*::*bgaB*) plasmid. The Agr reporter plasmid was constructed by amplifying the *bgaB* ORF from *Geobacillus stearothermophilus*, contained in pDL (53), using the primers Bga11 and Bga12. The resulting amplicon and pGID128 were separately digested using the restriction enzymes BglII (Thermo Fisher). The digested DNA was ligated using T4 ligase (Promega) and subsequently transformed into *E. coli* One Shot TOP10 (Invitrogen). The resulting plasmid was named pGID310-P$_{agrB}$::*gfp*::*bgaB*.

Bacterial transformation with σ^B and Agr reporter plasmids. *L. monocytogenes* electrocompetent cells were created as previously described (54). Cells were transformed with either pKSV7-P$_{lmo2230}$::*egfp* (30) or pGID310-P$_{agrB}$::*gfp*::*bgaB*. Transformed colonies were selected from BHI agar plates containing Chl and incubated at 30°C. Chromosomal integration of the plasmids was carried out as achieved as previously described (30), by incubating fluorescent cells at 42°C. The pKSV7-P$_{lmo2230}$::*egfp* chromosomal integration occurred upstream of the original P$_{lmo2230}$ through homologous recombination and pGID310-P$_{agrB}$::*gfp*::*bgaB* integrated upstream of the original P$_{agrB}$. Integration was verified by colony PCR using the forward primers *egfp-lmo2230*-F for pKSV7-P$_{lmo2230}$::*egfp* and *bgaB_agrB*_F for pGID310-P$_{agrB}$::*gfp*::*bgaB* in conjugation with the reverse primer *egfp/bgaB_lmo2230*_R for both plasmids.

Western blots for eGFP protein. *L. monocytogenes* EGD-e wild-type, Δ*sigB*, Δ*agrA*, and mutant strains, obtained during the *in vitro* evolution experiment at 42°C and 30°C, were grown to stationary phase at 37°C, and the total protein fractions were extracted. Cultures were supplemented with Tet and centrifuged at 9,000 × *g* for 15 min at 4°C. Pellets were resuspended in sonication buffer (13 mM Tris-HCl, 0.123 mM EDTA, and 10.67 mM $MgCl_2$, adjusted to pH 8.0). Bacterial suspensions were digested

with 1 mg · mL^{-1} of lysozyme (Sigma) for 30 min, centrifuged once more, and resuspended in sonication buffer. Resuspensions were then transferred into cryotubes containing zirconia-silica beads (Thistle Scientific) and bead beaten in a FastPrep-24 at a speed of 6 m · s^{-1} for 40 s, twice. Cell lysates were centrifuged at 13,000 × *g* for 30 min at 4°C, and the supernatant was recovered. Total protein quantification was performed using Pierce BCA protein assay kit (Thermo Scientific) according to the manufacturer's recommendations. Total protein concentrations were adjusted to a final concentration of 0.5 mg · mL^{-1} and 12 μL. Each sample was separated by SDS-PAGE (15% acrylamide/bis-acrylamide) along with the PageRuler Plus prestained protein ladder (Thermo Scientific). Protein was transferred onto a polyvinylidene difluoride (PVDF) membrane and blocked with Tris-buffered saline supplemented with 0.1% (vol/vol) Tween 20 (Sigma) (TBST) supplemented with 3% (wt/vol) skim milk powder (Sigma). SDS-PAGE gels were stained with GelCode Blue staining reagent (Thermo Scientific) and later destained in distilled water. Immunoblots were probed with rabbit polyclonal IgG anti-GFP antibodies (Santa Cruz Biotechnology) diluted 1:500 in TBST and incubated overnight at 4°C. The secondary antibody mouse anti-rabbit IgG-horseradish peroxidase (HRP) (Santa Cruz Biotechnology) was diluted to a 1:6,500 ratio in TBST and incubated with the membrane at room temperature (RT) for 1 h. Immunoblots were visualized in the Odyssey Fc imaging system (Li-Cor Biosciences). Band intensity was registered and quantified in Image Studio Lite version 5.2. Results are presented as a percentage of relative eGFP protein. Two biological replicates were made.

Qualitative analysis of the *agr* activity. *L. monocytogenes* EGD-e wild-type, Δ*sigB*, Δ*agrA*, and mutant strains obtained during the IVEE at 30°C and transformed with pGID310 were grown overnight in BHI supplemented with Chl at 30°C and streaked in BHI agar plates supplemented with X-Gal 0.1 mg · mL^{-1} (Thermo Scientific) and incubated at 30°C, 37°C, or 42°C. White or blue colony coloration was registered after 48 h of incubation.

***In vitro* competition experiments.** *L. monocytogenes* EGD-e wild-type, Δ*sigB*, Δ*agrA*, and mutant strains obtained during the IVEE at both temperatures were grown overnight in BHI at either 30°C or 37°C. Competitions experiments were carried out as previously described (21). Briefly, stationary phase cultures were adjusted to an initial optical density at 600 nm (OD_{600}) of 0.05 in fresh BHI medium at final ratios of 1:1 and incubated at the indicated temperatures. Passages were made every 24 h by diluting the cultures 1:100 into fresh BHI medium for 5 days. Samples were taken in every passage, diluted to 10^{-7} in PBS, plated onto BHI plates, and incubated at 37°C for 24 h and further incubated at 30°C for 5 days. Relative abundance was calculated.

Scanning electron microscopy. Overnight cultures of *L. monocytogenes* EGD-e wild-type, Δ*sigB*, and Δ*agrA* strains were diluted and plated in BHI agar plates at a concentration of 10^2 CFU · mL^{-1}. Plates were incubated at 37°C for 24 h and further incubated at 30°C for 6 days. Squares of approximately 1 cm^2 were cut from the agar containing a single colony and submerged in electron microscopy (EM) fixative buffer (2% glutaraldehyde + 2% paraformaldehyde in 0.1 M sodium cacodylate buffer, pH 7.2) for 2 h at RT. EM fixative buffer was replaced by 0.2 M sodium cacodylate (pH 7.2) and stored at 4°C until further processed. Samples were dehydrated for 15 min in successive immersions in increasing concentrations of ethanol (30%, 50%, 70%, 90%, and 100%), twice per concentration. Samples were then dried by critical point drying (Leica EM CPD300) and sputter-coated with gold (Quorum Q150R ES Plus). Samples were visualized in SEM (Hitachi S2600N). Three biological replicates were made.

***In silico* analysis of premature stop codon occurrence rates.** Methodology for this analysis was directly adapted from our previous study (21), however, with 40,080 genome sequences available from the NCBI database analyzed (accessed 19 April 2021). Briefly, a BLAST DNA database was constructed for each genome, and a BLASTN match for each gene of interest was extracted and translated *in silico*. For the genes determined as present in the genome, lengths of deduced translation products were calculated as percentage values relative to the length of reference protein sequence from the *L. monocytogenes* EGD-e strain. PMSC is defined as <90% of reference protein length and its occurrence as a rate corrected for gene length. In addition to the 41 genes previously analyzed, *agrBDCA* and all 31 genes encoding two-component systems, histidine kinases, or response regulators are included (55). The gene *lmo1508* that encodes for a histidine kinase is among MLST genes and is, thus, presented only in the two-component systems group (Fig. 6). Two of the two-component system-encoding genes (*lmo1060* and *lmo1061*) were excluded from Fig. 6, as it is absent in strains from *L. monocytogenes* lineage I.

RT-qPCR. Cultures of *L. monocytogenes* EGD-e wild-type, Δ*sigB*, Δ*agrA*, and Δ*sigB* Δ*agrA* double mutant strains were grown in BHI to mid-log phase (OD_{600} = 0.4) at 30°C. For analysis on field isolates, strains were grown in BHI to stationary phase at 37°C. RNAlater (Sigma) was used to stop the transcription. Extraction of total RNA was made with RNeasy minikit (Qiagen) according to the manufacturer's recommendations. Cells lysis was achieved by bead beating twice in a FastPrep-24 at a speed of 6 m · s^{-1} for 40 s. DNA was digested with Turbo DNA-free (Invitrogen) according to the manufacturer's recommendations. RNA integrity was verified by 0.7% agarose gel electrophoresis. SuperScript III first-strand synthesis system (Invitrogen) was used to synthesize cDNA according to the manufacturer's recommendations and further quantified using Qubit (Invitrogen). RT-qPCR was performed using a QuantiTect SYBR green PCR kit (Qiagen) and primers for the target genes (Table 3). Primer efficiencies for the target genes, 16S, *lmo2230*, *agrA*, and *agrB*, were determined using purified *L. monocytogenes* gDNA. Samples were analyzed on a LightCycler 480 system (Roche) with the following parameters: 95°C for 15 min; 45 cycles of 15 s at 95°C, 15 s at 53°C, and 30 s at 72°C; a melting curve drawn for 5 s at 95°C and 1 min at 55°C followed by increases of 0.11°C · s^{-1} until 95°C was reached; and cooling for 30 s at 40°C. Cycle quantification was calculated by using LightCycler 480 software version 1.5.1 (Roche) and the Pfaffl relative expression formula (56, 57). 16S rRNA expression was used as a reference. Three biological replicates were performed. Results were converted to Log_2 expression normalized relative to the WT strain.

Growth kinetics. Several *L. monocytogenes* strains were grown to stationary phase in BHI medium at 30°C and were adjusted to an initial OD_{600} of 0.05 and grown in fresh BHI medium at 30°C. Measurements of the OD_{600} of each culture were made every hour for 8 h. Growth rates were calculated with GrowthRates 4.3 software (58). Two biological replicates were made.

Biofilm formation. *L. monocytogenes* strains were grown overnight in BHI at 30°C. Cultures were diluted 1:100 into 50-mL conical bottom flasks containing 5 mL fresh BHI and further incubated for 24 h. Liquid cultures were discarded, washed twice with PBS, and dried at RT for 30 min. Flasks were dyed with 1% crystal violet (Sigma-Aldrich) for 30 min at RT and further washed twice with PBS and once with deionized water. Flasks were dried overnight at RT, and pictures were taken. Two biological replicates were made.

Statistical analysis. All pairwise comparisons for statistical significance were performed using a Student's *t* test. These analyses were performed using GraphPad Prism 8. *P* values of <0.05 (*), <0.01 (**), and <0.001 (***) were considered statistically significant.

Data availability. Whole-genome sequencing data is available on NCBI under BioProject accession numbers PRJNA371539, PRJNA808240, PRJNA699172, PRJNA714047, and PRJNA818619.

SUPPLEMENTAL MATERIAL

Supplemental material is available online only.

SUPPLEMENTAL FILE 1, PDF file, 0.6 MB.

ACKNOWLEDGMENTS

We thank members of the PATHSENSE network (https://www.pathsense.eu/) for helpful discussions throughout this study.

This project has received funding from the European Union's Horizon 2020 research-and-innovation program under Marie Skłodowska-Curie grant agreement no. 721456. Jialun Wu was funded by the Department of Agriculture, Food and the Marine (17/F/244).

REFERENCES

1. Hafner L, Pichon M, Burucoa C, Nusser SHA, Moura A, Garcia-Garcera M, Lecuit M. 2021. Listeria monocytogenes faecal carriage is common and depends on the gut microbiota. Nat Commun 12:6826. https://doi.org/10.1038/s41467-021-27069-y.
2. NicAogáin K, O'Byrne CP. 2016. The role of stress and stress adaptations in determining the fate of the bacterial pathogen Listeria monocytogenes in the food chain. Front Microbiol 7:1865. https://doi.org/10.3389/fmicb.2016.01865.
3. World Health Organization. 2018. Listeriosis. World Health Organization, Geneva, Switzerland. https://www.who.int/news-room/fact-sheets/detail/listeriosis. Accessed 2 June 2021.
4. Gaballa A, Guariglia-Oropeza V, Wiedmann M, Boor KJ. 2019. Cross talk between SigB and PrfA in Listeria monocytogenes facilitates transitions between extra- and intracellular environments. Microbiol Mol Biol Rev 83:e00034-19. https://doi.org/10.1128/MMBR.00034-19.
5. Sleator RD, Watson D, Hill C, Gahan CGMY. 2009. The interaction between Listeria monocytogenes and the host gastrointestinal tract. Microbiology (Reading) 155:2463–2475. https://doi.org/10.1099/mic.0.030205-0.
6. Tiensuu T, Guerreiro DN, Oliveira AH, O'Byrne C, Johansson J. 2019. Flick of a switch: regulatory mechanisms allowing Listeria monocytogenes to transition from a saprophyte to a killer. Microbiology (Reading) 165:819–833. https://doi.org/10.1099/mic.0.000808.
7. Guerreiro DN, Arcari T, O'Byrne CP. 2020. The σB-mediated general stress response of Listeria monocytogenes: life and death decision making in a pathogen. Front Microbiol 11:1505. https://doi.org/10.3389/fmicb.2020.01505.
8. Liu Y, Orsi RH, Gaballa A, Wiedmann M, Boor KJ, Guariglia-Oropeza V. 2019. Systematic review of the Listeria monocytogenes σB regulon supports a role in stress response, virulence and metabolism. Future Microbiol 14:801–828. https://doi.org/10.2217/fmb-2019-0072.
9. Kim H, Marquis H, Boor KJ. 2005. σB contributes to Listeria monocytogenes invasion by controlling expression of inlA and inlB. Microbiology (Reading) 151:3215–3222. https://doi.org/10.1099/mic.0.28070-0.
10. Ireton K, Cossart P. 1997. Host-pathogen interactions during entry and actin-based movement of Listeria monocytogenes. Annu Rev Genet 31:113–138. https://doi.org/10.1146/annurev.genet.31.1.113.
11. Lecuit M, Vandormael-Pournin S, Lefort J, Huerre M, Gounon P, Dupuy C, Babinet C, Cossart P. 2001. A transgenic model for listeriosis: role of internalin in crossing the intestinal barrier. Science 292:1722–1725. https://doi.org/10.1126/science.1059852.
12. Mengaud J, Ohayon H, Gounon P, Mège R-M, Cossart P. 1996. E-cadherin is the receptor for internalin, a surface protein required for entry of L. monocytogenes into epithelial cells. Cell 84:923–932. https://doi.org/10.1016/s0092-8674(00)81070-3.
13. Shen Y, Naujokas M, Park M, Ireton K. 2000. InlB-dependent internalization of Listeria is mediated by the Met receptor tyrosine kinase. Cell 103:501–510. https://doi.org/10.1016/S0092-8674(00)00141-0.
14. Oliveira AH, Tiensuu T, Guerreiro DN, Tükenmez H, Dessaux C, García-del Portillo F, O'Byrne C, Johansson J. 2022. Listeria monocytogenes requires the RsbX protein to prevent SigB activation under non-stressed conditions. J Bacteriol 204:e0048621. https://doi.org/10.1128/JB.00486-21.
15. Xia Y, Xin Y, Li X, Fang W. 2016. To modulate survival under secondary stress conditions, Listeria monocytogenes 10403S employs RsbX to downregulate σB activity in the poststress recovery stage or stationary phase. Appl Environ Microbiol 82:1126–1135. https://doi.org/10.1128/AEM.03218-15.
16. Ferreira A, Gray M, Wiedmann M, Boor KJ. 2004. Comparative genomic analysis of the sigB operon in Listeria monocytogenes and in other Gram-positive bacteria. Curr Microbiol 48:39–46. https://doi.org/10.1007/s00284-003-4020-x.
17. O'Byrne CP, Karatzas KAG. 2008. Advances in applied microbiology. Academic Press, San Diego, CA.
18. Brøndsted L, Kallipolitis BH, Ingmer H, Knöchel S. 2003. kdpE and a putative RsbQ homologue contribute to growth of Listeria monocytogenes at high osmolarity and low temperature. FEMS Microbiology Lett 219:233–239. https://doi.org/10.1016/S0378-1097(03)00052-1.
19. Chaturongakul S, Boor KJ. 2004. RsbT and RsbV contribute to σB-dependent survival under environmental, energy, and intracellular stress conditions in Listeria monocytogenes. Appl Environ Microbiol 70:5349–5356. https://doi.org/10.1128/AEM.70.9.5349-5356.2004.
20. O'Donoghue B, NicAogáin K, Bennett C, Conneely A, Tiensuu T, Johansson J, O'Byrne C. 2016. Blue-light inhibition of Listeria monocytogenes growth is mediated by reactive oxygen species and is influenced by σB and the blue-light sensor Lmo0799. Appl Environ Microbiol 82:4017–4027. https://doi.org/10.1128/AEM.00685-16.
21. Guerreiro DN, Wu J, Dessaux C, Oliveira AH, Tiensuu T, Gudynaite D, Marinho CM, Boyd A, García-Del Portillo F, Johansson J, O'Byrne CP. 2020. Mild stress conditions during laboratory culture promote the proliferation of mutations that negatively affect sigma B activity in Listeria monocytogenes. J Bacteriol 202:e00751-19. https://doi.org/10.1128/JB.00751-19.

22. Cao M, Bitar AP, Marquis H. 2007. A mariner-based transposition system for Listeria monocytogenes. Appl Environ Microbiol 73:2758–2761. https://doi.org/10.1128/AEM.02844-06.
23. Arnaud M, Chastanet A, Débarbouillé M. 2004. New vector for efficient allelic replacement in naturally nontransformable, low-GC-content, Gram-positive bacteria. Appl Environ Microbiol 70:6887–6891. https://doi.org/10.1128/AEM.70.11.6887-6891.2004.
24. Zetzmann M, Sánchez-Kopper A, Waidmann MS, Blombach B, Riedel CU. 2016. Identification of the agr peptide of Listeria monocytogenes. Front Microbiol 7:989. https://doi.org/10.3389/fmicb.2016.00989.
25. Garmyn D, Augagneur Y, Gal L, Vivant A-L, Piveteau P. 2012. Listeria monocytogenes differential transcriptome analysis reveals temperature-dependent Agr regulation and suggests overlaps with other regulons. PLoS One 7:e43154. https://doi.org/10.1371/journal.pone.0043154.
26. Riedel CU, Monk IR, Casey PG, Waidmann MS, Gahan CGM, Hill C. 2009. AgrD-dependent quorum sensing affects biofilm formation, invasion, virulence and global gene expression profiles in Listeria monocytogenes. Mol Microbiol 71:1177–1189. https://doi.org/10.1111/j.1365-2958.2008.06589.x.
27. Rieu A, Lemaître J-P, Guzzo J, Piveteau P. 2008. Interactions in dual species biofilms between Listeria monocytogenes EGD-e and several strains of Staphylococcus aureus. Int J Food Microbiol 126:76–82. https://doi.org/10.1016/j.ijfoodmicro.2008.05.006.
28. Dorey A, Marinho C, Piveteau P, O'Byrne C. 2019. Role and regulation of the stress activated sigma factor sigma B (σB) in the saprophytic and host-associated life stages of Listeria monocytogenes, p 1–48. *In* Gadd GM, Sariaslani S (ed), Advances in applied microbiology. Academic Press, San Diego, CA.
29. Marinho CM, Garmyn D, Gal L, Brunhede MZ, O'Byrne C, Piveteau P. 2020. Investigation of the roles of AgrA and σB regulators in Listeria monocytogenes adaptation to roots and soil. FEMS Microbiology Lett 367:fnaa036. https://doi.org/10.1093/femsle/fnaa036.
30. Utratna M, Cosgrave E, Baustian C, Ceredig R, O'Byrne C. 2012. Development and optimization of an EGFP-based reporter for measuring the general stress response in Listeria monocytogenes. Bioeng Bugs 3:93–103. https://doi.org/10.4161/bbug.19476.
31. Lauderdale KJ, Boles BR, Cheung AL, Horswill AR. 2009. Interconnections between Sigma B, agr, and proteolytic activity in Staphylococcus aureus biofilm maturation. Infect Immun 77:1623–1635. https://doi.org/10.1128/IAI.01036-08.
32. Gray J, Chandry PS, Kaur M, Kocharunchitt C, Fanning S, Bowman JP, Fox EM. 2021. Colonisation dynamics of Listeria monocytogenes strains isolated from food production environments. Sci Rep 11:12195. https://doi.org/10.1038/s41598-021-91503-w.
33. Rieu A, Weidmann S, Garmyn D, Piveteau P, Guzzo J. 2007. Agr system of Listeria monocytogenes EGD-e: role in adherence and differential expression pattern. Appl Environ Microbiol 73:6125–6133. https://doi.org/10.1128/AEM.00608-07.
34. Kumar S, Parvathi A, George J, Krohne G, Karunasagar I, Karunasagar I. 2009. A study on the effects of some laboratory-derived genetic mutations on biofilm formation by Listeria monocytogenes. World J Microbiol Biotechnol 25:527–531. https://doi.org/10.1007/s11274-008-9919-8.
35. Larsen MH, Kallipolitis BH, Christiansen JK, Olsen JE, Ingmer H. 2006. The response regulator ResD modulates virulence gene expression in response to carbohydrates in Listeria monocytogenes. Mol Microbiol 61:1622–1635. https://doi.org/10.1111/j.1365-2958.2006.05328.x.
36. Wu J, NicAogáin K, McAuliffe O, Jordan K, O'Byrne CP. 2022. Phylogenetic and phenotypic analyses of a collection of food and clinical *Listeria monocytogenes* isolates reveal loss of function of sigma B from several clonal complexes. Appl Environ Microbiol e00051-22. https://doi.org/10.1128/aem.00051-22.
37. Asakura H, Kawamoto K, Okada Y, Kasuga F, Makino S, Yamamoto S, Igimi S. 2012. Intrahost passage alters SigB-dependent acid resistance and host cell-associated kinetics of Listeria monocytogenes. Infect Genet Evol 12:94–101. https://doi.org/10.1016/j.meegid.2011.10.014.
38. O'Donoghue B. 2016. A molecular genetic investigation into stress sensing in the food-borne pathogen Listeria monocytogenes: roles for RsbR and its paralogues. Doctoral Thesis. National University of Ireland, Galway, Ireland.
39. Quereda JJ, Pucciarelli MG, Botello-Morte L, Calvo E, Carvalho F, Bouchier C, Vieira A, Mariscotti JF, Chakraborty T, Cossart P, Hain T, Cabanes D, García-del Portillo F. 2013. Occurrence of mutations impairing sigma factor B (SigB) function upon inactivation of Listeria monocytogenes genes encoding surface proteins. Microbiology (Reading) 159:1328–1339. https://doi.org/10.1099/mic.0.067744-0.
40. Connolly JPR, Roe AJ, O'Boyle N. 2021. Prokaryotic life finds a way: insights from evolutionary experimentation in bacteria. Crit Rev Microbiol 47:126–140. https://doi.org/10.1080/1040841X.2020.1854172.
41. Becker LA, Çetin MS, Hutkins RW, Benson AK. 1998. Identification of the gene encoding the alternative sigma factor σB from Listeria monocytogenes and its role in osmotolerance. J Bacteriol 180:4547–4554. https://doi.org/10.1128/JB.180.17.4547-4554.1998.
42. Guldimann C, Guariglia-Oropeza V, Harrand S, Kent D, Boor KJ, Wiedmann M. 2017. Stochastic and differential activation of σB and PrfA in Listeria monocytogenes at the single cell level under different environmental stress conditions. Front Microbiol 8:348. https://doi.org/10.3389/fmicb.2017.00348.
43. Robinson T, Smith P, Alberts ER, Colussi-Pelaez M, Schuster M. 2020. Cooperation and cheating through a secreted aminopeptidase in the Pseudomonas aeruginosa RpoS response. mBio 11:e03090-19. https://doi.org/10.1128/mBio.03090-19.
44. Spira B, de Almeida Toledo R, Maharjan RP, Ferenci T. 2011. The uncertain consequences of transferring bacterial strains between laboratories - rpoS instability as an example. BMC Microbiol 11:248. https://doi.org/10.1186/1471-2180-11-248.
45. Marinho CM, Dos Santos PT, Kallipolitis BH, Johansson J, Ignatov D, Guerreiro DN, Piveteau P, O'Byrne CP. 2019. The σB-dependent regulatory sRNA Rli47 represses isoleucine biosynthesis in Listeria monocytogenes through a direct interaction with the ilvA transcript. RNA Biol 16:1424–1437. https://doi.org/10.1080/15476286.2019.1632776.
46. García-Contreras R, Nuñez-López L, Jasso-Chávez R, Kwan BW, Belmont JA, Rangel-Vega A, Maeda T, Wood TK. 2015. Quorum sensing enhancement of the stress response promotes resistance to quorum quenching and prevents social cheating. ISME J 9:115–125. https://doi.org/10.1038/ismej.2014.98.
47. George SE, Hrubesch J, Breuing I, Vetter N, Korn N, Hennemann K, Bleul L, Willmann M, Ebner P, Götz F, Wolz C. 2019. Oxidative stress drives the selection of quorum sensing mutants in the Staphylococcus aureus population. Proc Natl Acad Sci U S A 116:19145–19154. https://doi.org/10.1073/pnas.1902752116.
48. Whiteley M, Diggle SP, Greenberg EP. 2017. Progress in and promise of bacterial quorum sensing research. Nature 551:313–320. https://doi.org/10.1038/nature24624.
49. Lee Y-J, Wang C. 2020. Links between S-adenosylmethionine and Agr-based quorum sensing for biofilm development in Listeria monocytogenes EGD-e. MicrobiologyOpen 9:e1015. https://doi.org/10.1002/mbo3.1015.
50. Tiensuu T, Andersson C, Rydén P, Johansson J. 2013. Cycles of light and dark co-ordinate reversible colony differentiation in Listeria monocytogenes. Mol Microbiol 87:909–924. https://doi.org/10.1111/mmi.12140.
51. Periasamy S, Joo H-S, Duong AC, Bach T-HL, Tan VY, Chatterjee SS, Cheung GYC, Otto M. 2012. How Staphylococcus aureus biofilms develop their characteristic structure. Proc Natl Acad Sci U S A 109:1281–1286. https://doi.org/10.1073/pnas.1115006109.
52. Deatherage DE, Barrick JE. 2014. Identification of mutations in laboratory-evolved microbes from next-generation sequencing data using Breseq, p 165–188. *In* Sun L, Shou W (ed), Engineering and analyzing multicellular systems: methods and protocols. Springer, New York, NY.
53. Yuan G, Wong SL. 1995. Regulation of groE expression in Bacillus subtilis: the involvement of the sigma A-like promoter and the roles of the inverted repeat sequence (CIRCE). J Bacteriol 177:5427–5433. https://doi.org/10.1128/jb.177.19.5427-5433.1995.
54. Monk IR, Gahan CGM, Hill C. 2008. Tools for functional postgenomic analysis of Listeria monocytogenes. Appl Environ Microbiol 74:3921–3934. https://doi.org/10.1128/AEM.00314-08.
55. Williams T, Bauer S, Beier D, Kuhn M. 2005. Construction and characterization of Listeria monocytogenes mutants with in-frame deletions in the response regulator genes identified in the genome sequence. Infect Immun 73:3152–3159. https://doi.org/10.1128/IAI.73.5.3152-3159.2005.
56. Pfaffl MW. 2001. A new mathematical model for relative quantification in real-time RT–PCR. Nucleic Acids Res 29:e45. https://doi.org/10.1093/nar/29.9.e45.
57. Pfaffl MW, Georgieva TM, Georgiev IP, Ontsouka E, Hageleit M, Blum JW. 2002. Real-time RT-PCR quantification of insulin-like growth factor (IGF)-1, IGF-1 receptor, IGF-2, IGF-2 receptor, insulin receptor, growth hormone receptor, IGF-binding proteins 1, 2 and 3 in the bovine species. Domest Anim Endocrinol 22:91–102. https://doi.org/10.1016/S0739-7240(01)00128-X.

58. Hall BG, Acar H, Nandipati A, Barlow M. 2014. Growth rates made easy. Mol Biol Evol 31:232–238. https://doi.org/10.1093/molbev/mst187.
59. den Dunnen JT, Dalgleish R, Maglott DR, Hart RK, Greenblatt MS, McGowan-Jordan J, Roux A-F, Smith T, Antonarakis SE, Taschner PEM. 2016. HGVS recommendations for the description of sequence variants: 2016 update. Hum Mutat 37:564–569. https://doi.org/10.1002/humu.22981.
60. Leong D, NicAogáin K, Luque-Sastre L, McManamon O, Hunt K, Alvarez-Ordóñez A, Scollard J, Schmalenberger A, Fanning S, O'Byrne C, Jordan K. 2017. A 3-year multi-food study of the presence and persistence of Listeria monocytogenes in 54 small food businesses in Ireland. Int J Food Microbiol 249:18–26. https://doi.org/10.1016/j.ijfoodmicro.2017.02.015.
61. Hilliard A, Leong D, O'Callaghan A, Culligan EP, Morgan CA, DeLappe N, Hill C, Jordan K, Cormican M, Gahan CGM. 2018. Genomic characterization of Listeria monocytogenes isolates associated with clinical listeriosis and the food production environment in Ireland. Genes 9:171. https://doi.org/10.3390/genes9030171.